An Integrated Design Optimization for Monolithic Mechanical Amplifier in PZT Nano-Positioning Stage

Chien Jong Shih* and Kuang You Chen

Department of Mechanical and Electro-Mechanical Engineering, Tamkang University, Tamsui, Taiwan 251, R.O.C.

Abstract

In order to satisfy the accelerating nanotechnology of high-tech precision manufacturing, it is essential to develop the efficient integration of amplifying device producing very fine resolution. This paper proposes such a development using topological optimal synthesis to design a monolithic mechanical amplifying lever actuated by a PZT in single-axis nano-positioning stage. This one-piece compound compliant mechanism consists of an amplifier and nano-motion bed. The resultant amplifier yields to a larger magnification factor than that in original design. The completed design implementation shows that the presenting design optimization is practical to apply. In addition, it provides a creative computational aided design (CAD) environment and integrated design process for mechanical amplifier and nano-positioning stage.

Key Words: Topology Optimization, Mechanical Design, Precision Engineering, Compliant Mechanism

1. Introduction

High precision and positioning performances are extremely important along with the rapid growing of semiconductor, MEMS (Micro-Electro-Mechanical Systems) and precision manufacturing process [1]. Due to composing different structures and materials, popular used dual motion positioning stage, both motor actuated ball screw and linear slider for coarse motion, and associated piezoelectric parts for fine motion require high level but difficult control system. A development of integrating amplifying device [2] can directly expand the motion of nano stage that shows very convenient for control. Such the device assembly makes very fine resolution possible and meets accelerating nanotechnology in high-tech precision manufacturing.

The earlier effort of Yang et al. [3] applied the flexure structural mechanics to develop an amplifying device incorporated with piezoelectric actuated single-axis nano stage. Lee and Kim [4] also applied flexural mechanics and proposed a design of micro XY-stage. Ryu et al. [2] presented a flexure hinge based XYθ wafer stage with size optimization constrained by travel distance within 100 μm. Elmustafa and Lagally [5] applied finite element analysis (FEA) to study the behavior of nano-position stage guided by flexural-hinges. Another micro-stage presented by Dai et al. [6] using the FEA to analyze the behavior of a flexural hinge guided by nano-motion.

A monolithic structure contains flexures that gain its mobility from the flexibility of some or all of members, so called the compliant mechanism. Some existing realistic compliant mechanisms were designed by combining trial approaches and experiences. Recently, the pseudo-rigid-body model (PRBM) [7] provides a systematic method to analyze general compliant structures. Interesting readers can refer a historical development of compliant mechanisms to Chang and Wang [8] in which a four-bar compliant micro-mechanism in polyethylene (PU) material was presented. Fu [9] applied the PRBM that includes mechanical flexures and amplifying lever with size optimization in a nanometer positioning stage. Hsiao

*Corresponding author. E-mail: cjs@mail.tku.edu.tw

[10] adopted Fu's nano-resolution stage analyzed by FEA and tolerance design. Their continuous efforts establish the knowledge to the fundamental nano-resolution stage.

Topology optimization is an integrated methodology developed for the mechanism or structural synthesis. Sigmund [11] first introduced the micro displacement inverter and amplifier that were created by structural topological optimization. Huang and Lan [12] presented a micro mechanical amplifier coupled with a PZT actuator. Shih et al. [13] presented a system topological design process with multiple objectives optimization technique for the design of compliant micro gripper. It is concluded that the hinge-like locations created in topology optimization are the exact locations of the flexure hinges in monolithic compliant mechanism.

This paper refers to Fu's [9] demonstration of a single-axis nano-positioning stage including an amplifying lever actuated by a PZT. Fu applied the conventional mechanical design method and genetic algorithm for optimization. The design task and conditions and requirements of current work remain the same as Fu's work. The presented monolithic compliant amplifier has been redesign by topological synthesis [13] mounted on a flexural nano stage of one-bed foundation. This one-piece compound compliant mechanism consists of amplifier and nano-motion bed consequently analyzed by the FEA. Several valuable recipes are given in the paper to resolve some possible difficulties during practical process. The performance, strategy, and parameters are analyzed and discussed that shows the effectiveness of this CAD based process for the mechanical amplifying mechanism integrated in PZT nano-positioning stage.

2. Model of Nano-Resolution Stage

A completed nano-positioning stage [9] shown in Figure 1 contains a PZT actuator, an amplifying lever and a flexure motion stage. The horizontal distance between two hinges indicated as B is 46 mm. The height of the amplifier is 18 mm. Such a one-piece nano-motion stage with four double compound leaf springs and two notch hinges B are machined by wire electric discharge machining (EDM). A PZT actuator has been applied at location A. The whole stage is made of stainless steel SUS304 with density 7.92 g/cm^3, Young's modulus 190 GPa, Poisson ratio 0.29 and yielding strength 520 MPa. The design goals require high stiffness, more than 200 Hz natural frequency, and a maximum output stroke. Fu [9] applied the genetic algorithm for parametric optimization resulted in the maximum output stroke 135.8 nm (nanometer) with natural frequency 280.8 Hz. Additionally, the experimental work using a P-840.30 PZT obtained a maximum output stroke 109.8 nm and natural frequency 264.0 Hz.

Hsiao [10] conducted the FEA to Fu's nano-stage with total thickness 18.5 mm, spring rate 0.09×10^6 N/m of each leaf, and thrust 1 Newton at PZT actuator. The maximum output displacement is 206.0 nm; the static stiffness of stage is 4.85×10^6 N/m, and the natural frequency is 316.04 Hz. The above nano-resolution stage has been conducted by optimum design, experimental test and finite element simulation. In this research, the portion of nano-motion stage is not considered for any change. However, the shape and material distribution of the amplifying lever has been redesign by formal topology optimization technique. The next section presents the redesign amplifying lever integrated into PZT nano-positioning stage.

3. Integrated Design Optimization

3.1 Design Variables, Domain and Boundary Conditions

Figure 2 shows a general domain for topological

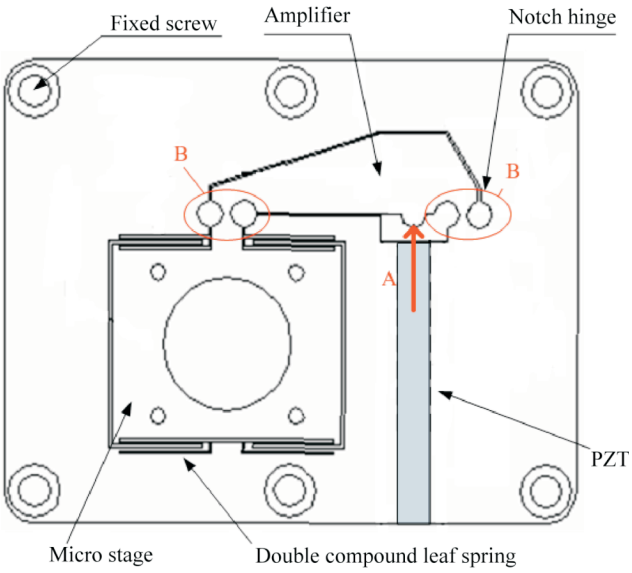

Figure 1. Original nano-stage model and loading.

structural design of a monolithic compliant mechanism. A spring with coefficient K_s at output port simulates the resistance from work-piece. It is critical to the formation of topology configuration [14]. The goal of the optimization problem is to maximize the work performed on the spring. In this paper, the design bound shown in Figure 3 presenting compliant magnifying mechanism that is identical to the configuration in Figure 1. The slant line at the right edge denotes the supported area. The output coefficient of soft spring is 0.36×10^6 N/m; and the coefficient of input spring is 20 times of output spring. The material is SUS304. An input force 1 Newton is applied at a distance of 9.5 mm from the center of the support area shown in Figure 3.

The design variable x_e represents the relative density of material in each finite element e that satisfies $\rho = x_e \rho_o$. The representation ρ_o means the original material density of a single element. A certain element is solid which means $x_e = 1$. In the SIMP model (solid isotropic microstructure with penalization) [14–16] the Young's modulus of each element can be represented in $E_e = (x_e)^{\alpha} E_o$, where α is a penalty factor. In order to obtain true "0-1" design, $\alpha \geq 3$ is usually required. In this work, $\alpha = 3$ is selected for study.

3.2 Mathematical Model of Topology Optimization

A topology optimization presented in this work, resolves the problem of distributing a limited amount of material in the design domain such that the output displacement is maximized, is formulated as follows.

$$\text{Maximize } f(X) = U_{y,out}(X) \tag{1}$$

$$\text{s.t. } \frac{\sum_{i=1}^{N} x_i}{N} - V_a \leq 0 \tag{2}$$

$$U_{x,out}^2(\boldsymbol{X}) / U_{y,out}^2(\boldsymbol{X}) \leq 0.01 \tag{3}$$

$$0.001 \leq x_i \leq 1 \tag{4}$$

The expression $U_{y,out}$ indicates vertical output displacement; and $U_{x,out}$ indicates horizontal output displacement. In the optimization process, the relation of $\{\boldsymbol{F}\} = [\boldsymbol{K}]\{\boldsymbol{U}\}$ must satisfy. The relative density in each element is a design variable. Eq. (2) indicates the material volume must be restricted within an allowable value V_a, as called control volume. In the Fu's result, the control volume is estimated around 64.2%. Therefore, the 60% for V_a in this study is used as constrained control volume. Since the useful output motion is vertical direction only; thus, Eq. (3) constrains the output displacement in horizontal direction is less than vertical direction.

3.3 Numerical Topology Optimization

The method of moving asymptotes (MMA) is adopted as the optimizer for optimum search [17,18] coupled with adjoint method for sensitivity analysis. In the solution process, the technique of a mesh-dependent filter is utilized to eliminate checkerboard-like phenomenon. The total finite element number used is 3744 (104 × 36). This multidisciplinary computational process is consequently summarized in the following algorithm.

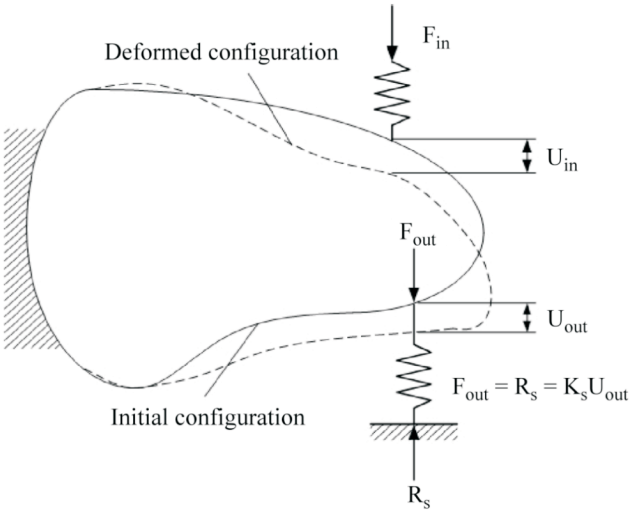

Figure 2. Domain of topology optimization for a compliant mechanism design.

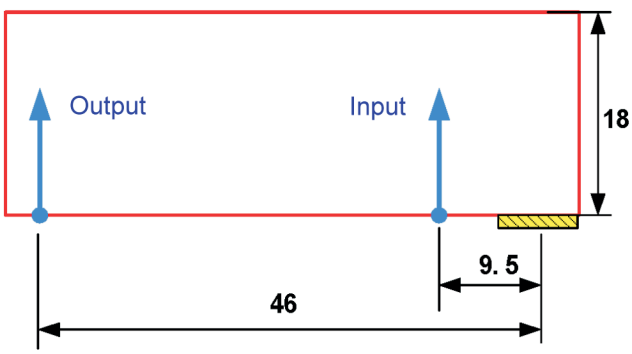

Figure 3. Design domain of amplifying mechanism using topology optimization (units are in mm).

(1) Perform the finite element analysis for structural stress, displacement, stiffness and natural frequency.
(2) Perform the sensitivity computation by applying adjoint method for the usage in numerical optimization.
(3) Apply the filter technique to eliminate the checkerboard occurrence which is generated in the finite element computation.
(4) Using asymptotes method to compose the approximate function for the mathematical formulation of topology optimization in MMA.
(5) Execute the numerical optimization using the algorithm of MMA.
(6) Examine the convergence. If the numerical result is converged, output the optimum topology and result. Otherwise, go to step 2 and the process is repeated.

The optimized topology synthesis can be obtained as shown in Figure 4. The maximum output of vertical displacement is 300.52 nm; the maximum output of horizontal displacement is 7.72 nm; the vertical input displacement is 61.0 nm, so that the magnification factor of vertical direction is 4.927.

3.4 Modification of Original Topology

The topology obtained in Figure 4 has a nice shape; however, the edges are not smooth and clear enough for practical use. Based on our knowledge of mechanical hinge, a modification can be treated after Figure 4 created. By the conclusion of Shih et al. [13], at the bottom right and above the support area there is a hinge-like flexure even it looks like a single point connection. The center of such a hinge at the support is then fixed so that the final modification of the amplifier with hinge area is presented in Figure 5. The distance of the input load from the hinge is 8.25 mm resulted from the outcome of topology optimization. The original range of 52 mm changes to 49.5 mm. The primary dimension of nano-motion bed is presented in Figure 6. The portion of the stage bed maintains the same as that in Fu's work. Consequently, a complete bed of nano stage connecting a compliant amplifying mechanism is shown in Figure 7 where an additional flexure hinge at the output portion is presented in Figure 8. One can see the space of 53 mm × 19 mm in Figure 7 is allowed for the machining and amplifier's motion. The length between two arcs on the flexure hinge is 1.5 mm that is same as that in Fu's study [9]. The radius of the arcs of flexure hinge is adopted as 2 mm. The different radius of arc is not as critical as the different distance between arcs in the sense of mechanical performance.

Figure 4. The final topological result of the amplifying mechanism ($V_a = 0.6$)

4. Performances Analysis of Nano Stage with Amplifier

Figure 9 indicates the displacement field of this

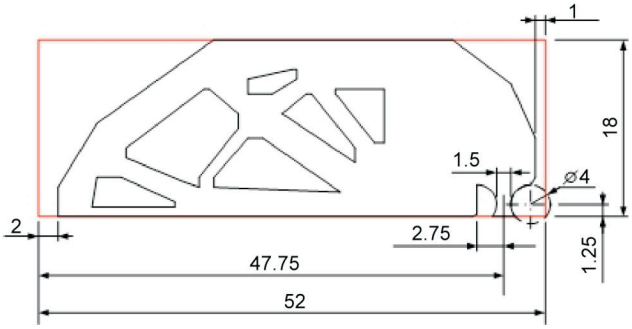

Figure 5. Modification of the amplifying mechanism of V_a = 0.6 after topology synthesis (units are in mm).

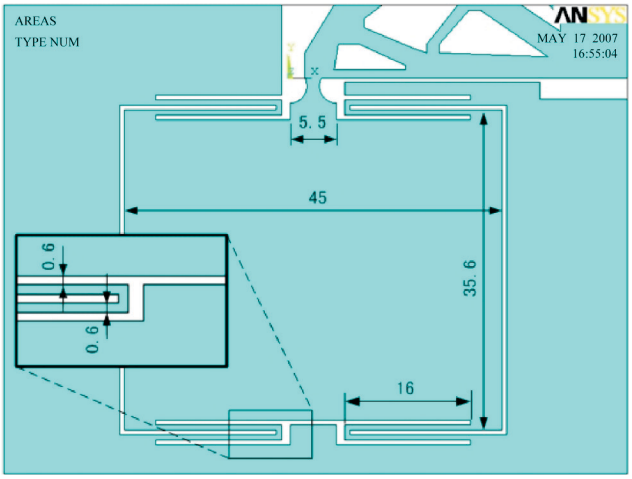

Figure 6. Nano-motion bed (units are in mm).

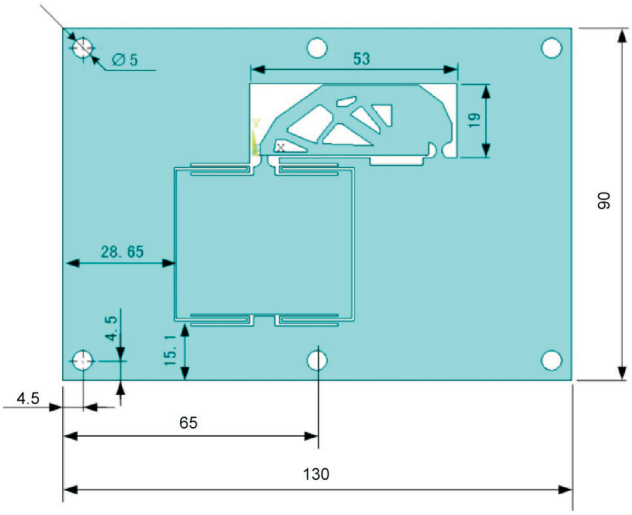

Figure 7. The assembly of the nano-stage (units are in mm).

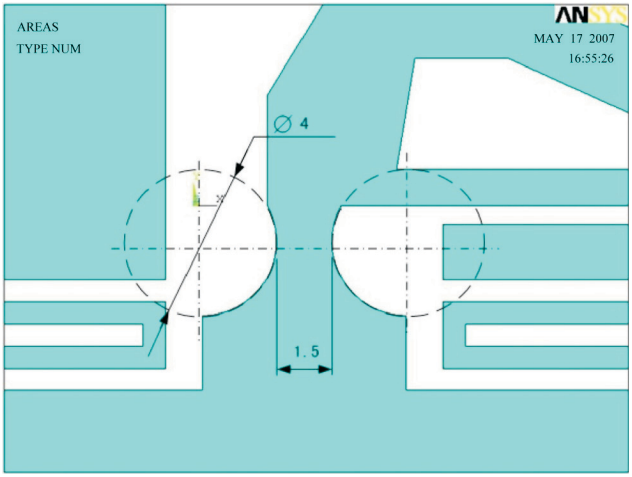

Figure 8. The neighborhood area of output hinge (units are in mm).

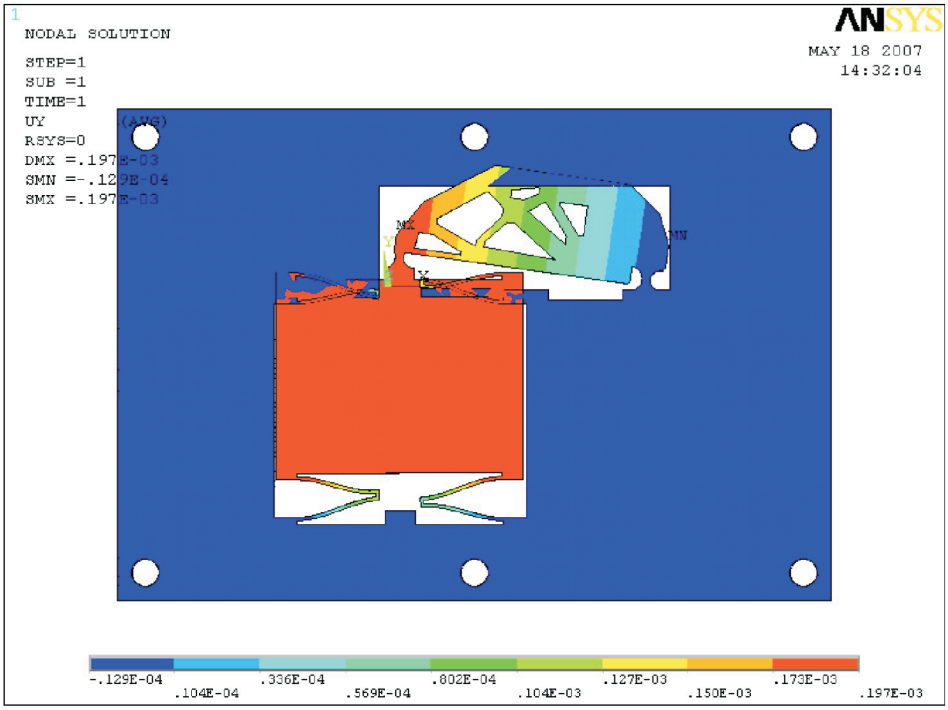

Figure 9. The displacement field of the nano stage assembly ($V_a = 0.6$).

nano stage assembly by ANSYS. The representation SMX means the maximum vertical displacement at the front head of amplifying mechanism. However, the useful point is the connection between the bed of nano-stage and amplifying lever. In there, a point with output vertical displacement is 192.58 nm and induced input vertical displacement is 42.19 nm using finite element analysis. Thus, the magnification ratio of output to input vertical displacement is 4.56.

The displacement field in Figure 9 not only shows the displacement observation corresponding to each point, critical location and magnification performance. It also provides information to produce the animation through digital computation technique. One can imagine the upper monolithic amplifier pull the nano-stage up and down through PZT actuation and the reaction of leaf springs. Since the motion is too small to observe the effective behavior in the animation through Figure 9.

Therefore, we enlarge the mobility scale that results in a out-of-plane distortion noted in Figure 9.

The static stiffness 5.19×10^6 N/m is obtained in this assembly stage. Since the horizontal displacement of output point is only 2.48 nm that is 1.28% of output vertical displacement. It is verified that the constraint of Eq. (3) is effective in proposed topology optimization. The maximum von Mises stress is 0.2124 MPa which occurs at the flexure hinge of input loading area. The fundamental natural frequency of the assembly stage is 318.8 Hz that is more than required 200 Hz.

When one compares the current design based on topological synthesis and the one presented in Fu [9] and Hsiao [10], Table 1 summarizes some properties and performances. The representation of $U_{y,in}$ indicates the input vertical displacement. M.F. means the magnification factor, i.e. the ratio of $U_{y,out}$ to $U_{y,in}$. The expression σ_e indicates the resulting maximum von Mises stress. Both results analyzed in this paper and Hsiao [10] show a good conformity. Additionally, the proposed topological basis design yields to a larger magnification factor (M.F.) than Hsiao. A larger vertical output displacement can be obtained by slightly moving applied load toward left. For example, when the applied load 1 Newton relocates at 11-mm away from the support hinge, the vertical output displacement becomes 257.66 nm. This significantly reveals that the location of the loading position can be simultaneously arranged while the structural material is redistributed. Consequently, the topology synthesis provides a more convenient and efficient way. Particularly, several topological outcomes can be generated through different control volume, boundary condition and material properties depending on designer's preference. Thus, the topology optimization can be an alternative synthesis methodology with much creativity and flexibility for monolithic compliant mechanism.

5. Post Design of Amplifying Mechanism

From Table 1 one knows that the maximum von Mises stress is much lower than yield strength 520 MPa. The material volume and weight of amplifier may be adjusted by either reducing the structural thickness or regulating control volume during the topology synthesis. This concept inspires and results in two experiments described as follows.

5.1 Reducing Thickness of Amplifier

Four amplifier thicknesses are studied: 18.5 mm, 15 mm, 10 mm and 5 mm. The distance between arcs on the flexure hinge is prescribed as 1.5 mm for both 18.5 mm and 15 mm. The distance between arcs on a flexure hinge is 2.0 mm for both 10 mm and 5 mm. The rest of parts of nano-stage assembly are the same as that in previous case. The resultant analysis by ANSYS is summarized in Table 2. One can see the magnification factor (M.F.) generally maintains similar for different structural thickness in this two-dimensional topology optimization. As long as the material strength is strong enough, a lighter weight mechanism is preferred for generating larger magnification factor and vertical output displacement.

5.2 Reducing Material Volume of Amplifier

In the primary design phase of topological synthesis, the control volume in Eq. (3) is constrained by:

$$\frac{\sum_{i=1}^{N} x_i}{N} - 0.3 \le 0 \tag{5}$$

Table 2. Performances of different amplifier thickness ($V_a = 0.6$)

Thickness (mm)	18.5	15	10	5
$U_{y,out}$ (nm)	192.58	235.69	282.10	530.32
$U_{x,out}$ (nm)	-2.48	-3.04	-3.79	-7.04
$U_{y,in}$ (nm)	42.19	51.05	62.83	113.81
M.F.	4.56	4.62	4.49	4.66
Max. σ_e (MPa)	0.2124	0.2599	0.3244	0.6269
ϖ_1 (Hz)	318.8	322.7	292.8	294.0

Table 1. Comparison of Hsaio [10] and presented topological basis design

	Volume	$U_{y,out}$ (nm)	$U_{x,out}$ (nm)	$U_{y,in}$ (nm)	M.F.	Stiffness (N/m)	ϖ_1 (Hz)	Max. σ_e (MPa)
Hsiao [10]	64.2%	206.0	/	/	/	4.85×10^6	316.04	/
Simulate [10]	64.2%	240.2	3.19	60.70	3.96	4.16×10^6	285.31	0.2596
$V_a = 0.6$	60%	192.58	2.48	42.19	4.56	5.19×10^6	318.8	0.2124

In this case of reducing control volume, the design domain is the same as Figure 3. All conditions are also the same as that in Section 3.1. The synthesis using topology optimization can be obtained as shown in Figure 10. The maximum vertical output displacement is 292.71 nm; the maximum horizontal output displacement is 6.74 nm; the input vertical displacement is 55.09 nm, so that the magnification factor of vertical displacement is 5.31.

The topology obtained in Figure 10 has a well layout. At the bottom right and above the support area, a single point connection shows the location of a hinge-like. A final configuration of amplifying mechanism after topology synthesis is modified and presented in Figure 11. The assembly of nano-stage is ready for ANSYS analysis including an additional flexure hinge located at output portion. The length between two arcs on the flexure hinge is 1.5 mm that is same as in previous study. The radius of the arcs of flexure hinge still matain 2 mm. The maximum vertical displacement at output and detailed hinge area is 214.98 nm. An induced vertical input displacement is 42.66 nm. Thus, the magnification factor of vertical to input displacement is 5.04. The static stiffness of this assembly stage can be obtained as 4.65×10^6 N/m. The horizontal displacement of output point is only 5.01 nm. The maximum von Mises stress is 0.2119 MPa which occurs at the flexure hinge of input loading area. The fundamental natural frequency of the assembly stage is 268.2 Hz that is more than required 200 Hz.

Figure 10. The final topological result of the amplifying mechanism ($V_a = 0.3$).

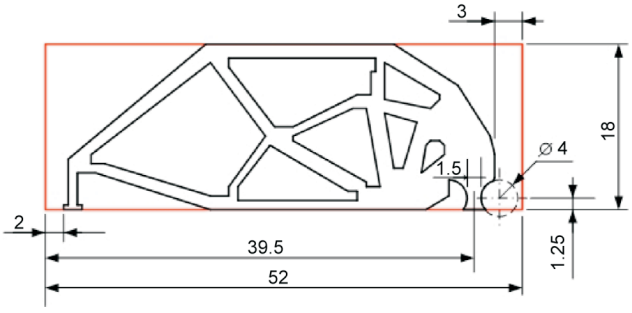

Figure 11. Modification of the amplifying mechanism of $V_a = 0.3$ after topology synthesis (units are in mm).

When one compares the current design based on the topological synthesis and the design presented in Fu [9] and Hsiao [10], Table 3 shows some properties and performance. Once more, four kinds of amplifier thickness (18.5 mm, 15 mm, 10 mm and 5 mm) are studied under $V_a = 0.3$. The distance between arcs on the flexure hinge is 1.5 mm for both 18.5 mm and 15 mm. The distance between arcs on a flexure hinge is 2.0 mm for both 10 mm and 5 mm. A larger distance between arcs can compensate the flexure rigidity due to the smaller structural thickness. The rest of parts in nano-stage assembly are the same. The results of ANSYS analysis are summarized in Table 4. One compares Table 2 and Table 4, both control volume and material thickness are significant to the resulting performances. A practical consideration of applying the proposed implementation is to repeat the computation by alternating those two factors until a satisfaction appears.

Table 4. Performances of different amplifier thickness ($V_a = 0.3$)

Thickness (mm)	18.5	15	10	5
$U_{y,out}$ (nm)	214.98	263.06	301.31	566.88
$U_{x,out}$ (nm)	5.01	6.14	6.70	12.83
$U_{y,in}$ (nm)	42.66	51.55	60.06	108.84
M.F.	5.04	5.10	5.02	5.21
Max. σ_e (MPa)	0.2119	0.2588	0.3266	0.6339
ϖ_1 (Hz)	268.2	267.7	299.9	296.1

Table 3. Comparison of presented topological basis design

	Volume	$U_{y,out}$ (μmm)	$U_{x,out}$ (μmm)	$U_{y,in}$ (μmm)	M.F.	Stiffness (N/m)	ϖ_1 (Hz)	Max. σ_e (MPa)
Hsiao [10]	64%	206.0	/	/	/	4.85×10^6	316.04	/
$V_a = 0.6$	60%	192.58	2.48	42.19	4.56	5.19×10^6	318.8	0.2124
$V_a = 0.3$	30%	214.98	5.01	42.66	5.04	4.65×10^6	268.2	0.2119

6. Concluding Remarks

Through the presented design and analysis, the topological synthesis is a very creative and effective method to generate alternative layout for a monolithic compliant mechanism, particularly for the design of mechanical amplifier. The resultant topological structure can yield to a maximum magnification factor and a satisfying output displacement. This paper demonstrates an integrated design process of designing a monolithic compliant amplifier for single-axis nano-positioning stage with an amplifying lever actuated by a PZT. As long as the strength based constraints and specified actuator meet the operation requirements, the presented implementation shows convenient and practical. A further study can be extend to three dimensions, simultaneously minimize compliance and weight, and includes stress constraints in one phase in the design optimization.

Acknowledgement

The support received from the National Science Council, Taiwan, under Grant No. NSC 96-2221-E-032-042, is gratefully acknowledged. We like to give a sincere thank and honor to Professor Krister Svanberg, Department of Mathematics, KTH, Sweden, for his kind support of the optimization of MMA.

References

[1] SIA, *The National Technology Roadmap for Semiconductor* (1997).

[2] Ryu, J. W., Gweon, D. G. and Moon, K. S., "Optimal Design of a Flexure Hinge Based XYθ Wafer Stage," *Precision Engineering*, Vol. 21, pp. 18–28 (1997).

[3] Yang, R., Jouaneh, M. and Schweizer, R., "Design and Characterization of a Low-Profile Microposioning Stage," *Precision Engineering*, Vol. 18, pp. 20–29 (1996).

[4] Lee, C. W. and Kim, S. W., "An Ultra-Precision Stage for Alignment of Wafers in Advanced Microlithography," *Precision Engineering*, Vol. 21, pp. 113–122 (1997).

[5] Elmustafa, A. A. and Lagally, M. G., "Flexural-Hinge Guided Motion Nanopositioner Stage for Precision Machining: Finite Element Simulation," *Precision Engineering*, Vol. 25, pp. 77–81 (2001).

[6] Dai, R., Xie, T. B. and Chang, S. P., "A Micro-Displacement Stage for Scanning White-Light Interferometry," *Journal of Physics: Conference Series*, Vol. 13, pp. 94–97 (2005).

[7] Howell, L. L., *Compliant Mechanisms*, John Wiley & Sons, New York, U.S.A. (2001).

[8] Chang, R. J. and Wang, Y. L., "Integration Method for Input-Output Modeling and Error Analysis of Four-Bar Polymer Compliant Micromachines," *Journal of Mechanical Design*, Vol. 121, pp. 220–228 (1999).

[9] Fu, S. J., "Optimal Design and Characterization of a Nanometer Poisoning Stage," *Master Thesis*, Department of Mechanical Engineering, Chun-Hsin University, Taiwan, ROC (2001).

[10] Hsiao, G. M., "Tolerance Design and Analysis of a Nano-Resolution Micro Stage," *Master Thesis*, Department of Mechanical Engineering, Chun-Hsin University, Taiwan, ROC (2004).

[11] Sigmund, O., "On the Design of Mechanisms Using Topology Optimization," *Mech. Struct. & Mach*., Vol. 25, pp. 493−524 (1997).

[12] Huang, S. C. and Lan, G. J., "Design and Fabrication of a Micro-Compliant Amplifier with a Topology Optimal Compliant Mechanism Integrated with a Piezoelectric Microactuator," *Journal of Micromechanics and Micro-Engineering*, Vol. 16, pp. 531−538 (2006).

[13] Shih, C. J., Lin, C. F. and Chen, H. Y., "An Integrated Design of Flexure Hinges and Topology Optimization for Monolithic Compliant Mechanism," *Journal of Integrated Design & Process Science*, Vol. 10, pp. 1−16 (2006).

[14] BendsØe, M. P. and Haber, R. B., "The Michell Layout Problem as a Low Volume Fraction Limit of the Perforated Plate Topology Optimization Problem: An Asymptotic Study," *Structural Optimization*, Vol. 6, pp. 263–267 (1993).

[15] Mlejnek, H. P. and Schirrmacher, R., "An Engineering's Approach to Optimal Material Distribution and Shape Finding," *Computer Method in Applied Mechanics and Engineering*, Vol. 106, pp. 1–26 (1993).

[16] Rozvany, G. I. N., "Aims, Scope, Methods, History and Unified Terminology of Computer-Aided Topology Optimization in Structural Mechanics," *Struct. Multidisc. Optim*., Vol. 21, pp. 90–108 (2001).

[17] Kirsch, U., *Structural Optimization*, Springer-Verlag (1993).

[18] Svanberg, K., "The Method of Moving Asymptotes - A New Method for Structural Optimization," *Int. J. Numer. Meth. Eng*., Vol. 24, pp.359–373 (1987).

Manuscript Received: Oct. 30, 2008
Accepted: Jun. 22, 2009